Fibers and Polymers 2017, Vol.18, No.2, 221-230
DOI 10.1007/s12221-017-6690-1

ISSN 1229-9197 (print version)
ISSN 1875-0052 (electronic version)

Antimicrobial Properties of Chitosan Nanoparticles: Mode of Action and Factors Affecting Activity

K. Divya, Smitha Vijayan, Tijith K. George, and M. S. Jisha*

School of Biosciences, Mahatma Gandhi University, Kottayam, Kerala-685560, India
(Received July 14, 2016; Revised November 16, 2016; Accepted November 18, 2016)

Abstract: The present investigation describes the synthesis and characterization of novel biodegradable nanoparticles based on chitosan for biomedical applications. The presence of primary amine groups in repeating units of chitosan grants it several properties like antibacterial activity, antitumor activity and so on. Chitosan forms nanoparticles spontaneously on the addition of polyanion tripolyphosphate which has greater antimicrobial activity than parent chitosan. In the present study, chitosan nanoparticles (ChNP) were prepared by the ionic gelation method. The physiochemical characteristics of nanoparticles were analyzed using XRD, SEM, FTIR. The antibacterial activity of chitosan nanoparticles against medical pathogens *Klebsiella pneumoniae, Escherichia coli, Staphylococcus aureus* and *Pseudomonas aeruginosa* was evaluated by calculation of minimum inhibitory concentration (MIC) and compared with chitosan and chitin activity. The mode of action and factors affecting antibacterial activity were also analyzed. ChNP compounds exhibited superior antimicrobial activity against all microorganisms in comparison with chitosan and chitin. The antibiofilm activity was studied using crystal violet assay and growth on congo red agar. The study is thus a good demonstration of the applicability of chitosan nanoparticles as an effective antimicrobial agent with antibiofilm activity as well.

Keywords: Antimicrobial property, Antibiofilm activity, Chitosan nanoparticles, Chitosan, TTC test

Introduction

The evolution of antibiotic resistant microorganisms has attracted much attention recently. It has been reported that there is no single antimicrobial agent that has not exhibited resistance by microorganisms [1]. This new development has forced scientists to formulate novel antimicrobial agents that show an effect against the continually increasing antibiotic resistant pathogenic microorganisms [2]. Chitosan has a new found popularity in this regard as bacteria are not reported to develop resistance to chitosan [3].

Chitosan is the second most abundant polysaccharide in nature. It is a linear polysaccharide of (1→4)-linked 2-acetamido-2-deoxy-beta-D-glucopyranose (GlcNAc) units and 2-amino-2-deoxy-beta-D-gulcopyranose (GlcN) units [4]. It is acclaimed for its nontoxic nature, biodegradability, polycationic, antimicrobial activity, antitumor activity, antioxidative activity, anticholesterolemic, hemostatic and analgesic effect [5-12]. Chitosan nanoparticle (ChNP) can be prepared easily by the incorporation of polyanion like tripolyphosphate (TPP) in chitosan solution under continuous stirring. These nanoparticles are found to have increased activity compared to the parent chitosan [13].

Chitosan exhibits a wide range of antimicrobial activity against bacteria, filamentous fungi, yeast and even virus. Studies have reported antibacterial activity of ChNP against *Escherichia coli, Staphylococcus aureus, Streptococcus mutans, Salmonella, typhimurium, Salmonella choleraesuis, Pseudomonas aeruginosa* [14-17]. Antifungal activity of CHNP has also been reported against *Aspergillus niger, Fusarium solani, Rhizoctonia solani, Collectotrichum gloeosporioides, Candida albicans* [13,18]. Antiviral activity of ChNP against Human cytomegalovirus (HMCV) strain AD-169, H1N1 Influenza A virus has also been reported recently [19,20].

Several studies have shown chitosan to exhibit higher antibacterial activity against gram positive bacteria than gram negative bacteria, while some other studies have shown that gram negative bacteria as more susceptible than gram positive [21,22]. Still many works have demonstrated that there is no significant difference between the antibacterial activity and bacterial species [23].

The exact mechanism of antibacterial activity is yet to be fully understood. The most prevalent proposed antibacterial activity of chitosan is by binding to the negatively charged bacterial cell wall causing disruption of the cell thus altering the membrane permeability, followed by attachment to DNA causing inhibition of DNA replication and subsequently cell death [24]. Another possible mechanism is that chitosan acts as a chelating agent that selectively binds to trace metal elements causing toxin production and inhibiting microbial growth [25].

The antibacterial activity of chitosan is also dependent on various factors both intrinsic and extrinsic. Intrinsic factors include the molecular weight and degree of deacetylation of parent chitosan, size and concentration of nanoparticle etc. The extrinsic factors include pH, temperature, reactive time and so on [26].

In the present study, we have synthesized and characterized ChNP by ionic gelation method. The antibacterial activity of ChNP against *Klebsiella pneumoniae, Escherichia coli, Staphylococcus aureus, P. aeruginosa* was evaluated. The

*Corresponding author: jishams@mgu.ac.in

mode of antibacterial activity was also briefly studied. We have also investigated the factors affecting the antibacterial activity of ChNP using a simple method of tetrazolium/ formazan test (TTC test). The activity of ChNP against biofilm formation of *K. pneumoniae, E. coli, S. aureus, P. aeruginosa* was also studied.

Experimental

Synthesis of Chitosan Nanoparticles

Chitosan nanoparticles were prepared using ionic gelation method [27]. Different concentrations of chitosan (1-5 mg) was added to 1 % acetic acid (v/v) and mixed well using magnetic stirrer. The ChNP were formed by adding 1 % TPP (w/v) drop by drop under magnetic stirring. Then the solution was centrifuged at 10,000 rpm for 10 minutes to remove residual TPP and the particles were freeze dried. Practical yield was calculated from the following equation [28].

$$\mathrm{PY}(\%) = \left[\frac{\text{Weight of nanoparticle}}{\text{Theoretical mass (Polymer + TPP)}}\right] \times 100 \quad (1)$$

Characterization of Chitosan Nanoparticles

XRD analysis of chitosan nanoparticle compounds was done to detect its crystallinity and particle size was calculated. A Bruker AXS D8 Advance diffractometer was used for the purpose. The size of nanoparticles was calculated using Debye Scherrer's equation.

$$d = \left[\frac{K\lambda}{\beta\cos\theta}\right] \quad (2)$$

where d is mean grain size, β is FWHM, λ is X-ray wavelength, θ is diffraction angle and k is Scherrer's constant with a value of 0.9. FTIR spectra of chitosan nanoparticles were taken with potassium bromide pellets on a Shimadzu IR Prestige 21 FTIR-ATR attached spectrometer.

The structure of chitosan nanoparticle compounds was examined using scanning electron microscope. The dried samples were mounted on specimen stubs with double adhesive tape and coated with platinum in a sputter coater and examined under JEOL 6390 SEM JSM at 10 kV.

AFM imaging was performed using Si3N4 probes with a spring constant of 0.06 N/m (APER-A-100SPM).

Assays for Antibacterial Activity

The antibacterial properties of ChNP were evaluated by a turbidimetric method against *K. pneumoniae* (MTCC 109), *E. coli* (MTCC 723), *S. aureus* (MTCC 734), *P. aeruginosa* (MTCC 121). The bacteria were cultured overnight in Muller-Hinton Broth (MHB) and the microbial suspension were adjusted to an OD_{600} of 1.0. Different concentrations (10 mg to 50 mg) of $ChNP_1$ (19 nm), $ChNP_2$ (21 nm), $ChNP_3$ (120 nm), $ChNP_4$ (153 nm) and $ChNP_5$ (165 nm) were suspended in sterile distilled water. The tubes were inoculated under aseptic conditions with 50 μl of the freshly prepared bacteria suspension. Cultures of ChNP free medium under same growth conditions were used as control. The MHB media without microorganism but containing the same concentration of ChNP were used as blank control. After mixing, the tubes were incubated at 37 °C for 24 h. The tubes were then studied for the visible signs of growth or turbidity. The lowest concentration of chitosan nanoparticles that inhibited the growth of bacteria was considered as the minimum inhibitory concentration or MIC. The OD of cultures were determined spectrophotometrically [2]. The percentage of inhibition was calculated as follows.

$$\text{Inhibition rate} = 1 - \left[\frac{\text{OD sample}}{\text{OD control}}\right] \times 100 \quad (3)$$

Zone of inhibition was checked by agar well diffusion method. For this, 1 ml fresh bacterial cultures were homogenously spread on solidified nutrient agar plates and 100 μl homogenized solutions of ChNP were filled in wells prepared by gel cutter. The plates were incubated at 37 °C for 24 h. Zone size was determined. Triplicates were kept [16].

Mechanism of Antibacterial Activity

Cell membrane integrity was evaluated by determining the release of cellular constituents at 260 nm. Cultured bacteria were harvested, washed, and resuspended in sterile 0.5 %NaCl solution. The cell suspension was adjusted to achieve an absorbance of 0.7 at 420 nm. 1.5 ml ChNP were mixed with 1.5 ml bacterial suspension suspensions at a ratio of 1:1 (v/v), and the absorbance at 260 nm was monitored using a UV spectrophotometer [29].

Factors Affecting Antibacterial Activity

Different parameters viz. temperature, reactive time and pH were compared for *K. pneuminiae* and *S. aureus* using tetrazolium/formazan test. In the presence of bacteria, TTC is reduced to red formazan. The intensity of the formazan produced is measured spectrophotometrically. This as an indicator of the activity and viability of cells.

TTC powder was dissolved in sterile distilled water at a concentration of 5 mg/ml at room temperature and then filtered through 0.22 μm Whatmann filter paper. 100 μl of different concentration of ChNP in 1 % acetic acid was poured in 40 ml nutrient growth medium containing 20 μl of 10^8 cells per ml challenge microorganism. The ChNP free solution was used as blank. All flasks were incubated at 37 °C with shaking at 200 g for 3 h. 1 ml from each flask was added to sterile test tubes containing 100 μl TTC solution (0.5 % w/v). All tubes were incubated at 37 °C for 20 min. The resultant formazan was centrifuged at 4000 g for 3 min. The supernatant was discarded and the pellets resuspended and centrifuged in 50 % ethanol. The red formazan solution obtained was measured using UV visible spectroscopy at 480 nm [30].

Biofilm Inhibition Assay

Chitosan nanoparticles were dissolved in sterile distilled water at different concentrations (100, 200, 300, 400 and 500 mg/m*l*), mixed well to obtain a complete homogenous mixture. Biofilm inhibition was carried out in 96 well plate. 100 μl of bacterial cell suspension was prepared in brain Heart Infusion Broth (BHIB) and added into 96 well titer plate and different concentrations of nanoparticles were added. Nanoparticle free cell suspension and uninoculated BHIB with nanoparticle served as positive and negative control. The plates were at incubated 37 °C for 3 days. After incubation, the broth was removed and washed thrice with sterile distilled water to remove unattached cells. 100 μl of 1 % (w/v) aqueous solution of crystal violet was added and kept for 30 minutes. The dye was removed and the wells were washed thoroughly and 95 % ethanol was added and incubated for 15 minutes. The reaction mixture was read spectrophotometrically at 570 nm [41]. Inhibition of biofilm formation was calculated using the formula below.

$$\text{Inhibition rate} = 1 - \left[\frac{\text{OD Treatment}}{\text{OD control}}\right] \times 100 \quad (4)$$

The growth on Congo Red Agar (CRA) was also studied. Glass bits were incubated in ChNP-BHIB inoculated with bacterial suspensions for 3 days. Glass bits incubated with ChNP free BHIB inoculated bacterial suspensions served as control. Glass bits were washed thrice in sterile distilled water and placed on CRA plates. The plates were incubated at 37 °C for 24 h. Black colonies indicated biofilm formation [42]. Triplicates were kept.

Results

Chitosan nanoparticles were formed by ionic interaction between negatively charged polyanion, tripolyphosphate and positively charged amino group (-NH_3) of chitosan [31]. The nanoparticles were formed spontaneously through the formation of intra and intermolecular cross-linkages under a constant stirring at ambient temperature. The ChNP obtained were freeze dried and stored for further use.

In the present study, the effect of concentration on the particle size of nanoparticles was investigated. A linear relation was observed such that lower the concentration of chitosan, smaller the size of ChNP. The decrease in size with concentration was reported in other works also. The practical yield of ChNP compounds was calculated and are shown in Table 1.

Table 1. Practical yield of CHNP compounds 1 (1 mg/m*l*), 2 (2 mg/m*l*), 3 (3 mg/m*l*), 4 (4 mg/m*l*), 5 (5 mg/m*l*)

Sl. no.	CHNP compound	Practical yield (%)
1	$ChNP_1$	36
2	$ChNP_2$	57
3	$ChNP_3$	76
4	$ChNP_4$	45
5	$ChNP_5$	55

Characterization of Chitosan Nanoparticles

The X-ray powder diffraction patterns of chitosan and ChNP compounds were recorded and are shown in Figure 1. The diffraction pattern of pure chitosan shows two peaks at 2θ=9.28 ° and 20.18 ° indicating the crystalline form II [16]. The peak at 2θ=18 ° found in XRD pattern of $ChNP_2$ and $ChNP_3$ is due to the presence of chitosan in nanoparticle [32]. The disappearance of the peak at angle 2θ=20 ° is found at higher chitosan concentrations. Broad bands are seen at 2θ= 30 °. Table 2 shows the size of nanoparticles calculated.

Scanning electron micrograph of ChNP (Figure 2) shows spherical shaped chitosan nanoparticles. There was no agglomeration observed in the nanoparticles. TEM images (Figure 3) shows nanoparticles having nearly spherical shape with a smooth surface and size range of about 20-70 nm. Atomic force micrograph (Figure 4) shows spherical shaped nanoparticles which are in agreement with the SEM image.

FTIR studies of ChNP were performed to analyze the chemical structure of nanoparticle. The FTIR spectrum is shown in Figure 5. A broad band between 3300-3200 cm^{-1} is observed. This indicates the presence of -OH and -NH_2 groups [16]. The peak at 2880 cm^{-1} corresponds to CH_2 groups. The peak at 1643 cm^{-1} corresponds to cross-linkage of ammonium groups within TPP molecules [17]. The peak at 1419 cm^{-1} corresponds to C-O stretching [2].

Antibacterial Activity

The antibacterial activity of different ChNP was evaluated against four different strains of medically important bacteria by determining the minimum inhibitory concentration (MIC) values and rate of inhibition. The rate of inhibition was calculated for each ChNP against the selected microorganism and MIC calculated. All the ChNP had high inhibition rates against tested microorganisms (Figure 6). The MIC of ChNP compounds were calculated from the rate of inhibition (Table 3). $ChNP_2$ and $ChNP_3$ showed more activity against the pathogens. $ChNP_3$ showed 85 % and 95 % rate of inhibition against *Klebsiella pneumoniae* and *Pseudomonas aeruginosa* at a concentration of 20 mg/m*l* and 10 mg/m*l* respectively. $ChNP_2$ inhibited 92 % and 85 % of *Staphylococcus aureus* and *Escherichia coli* at a concentration of 30 mg/m*l* and 40 mg/m*l* respectively. These concentrations of ChNP compounds were used in the qualitative analysis of antibacterial activity and zone of inhibition calculated. From the calculated zone of inhibition diameter, it was deducted that $ChNP_4$ had maximum activity against *S. aureus, P. aeruginosa* and *E. coli* while $ChNP_3$ had maximum activity against *K. pneumoniae*. The zone of inhibition of all ChNPs was higher than that of chitin and chitosan (Table 4). $ChNP_3$ produced a

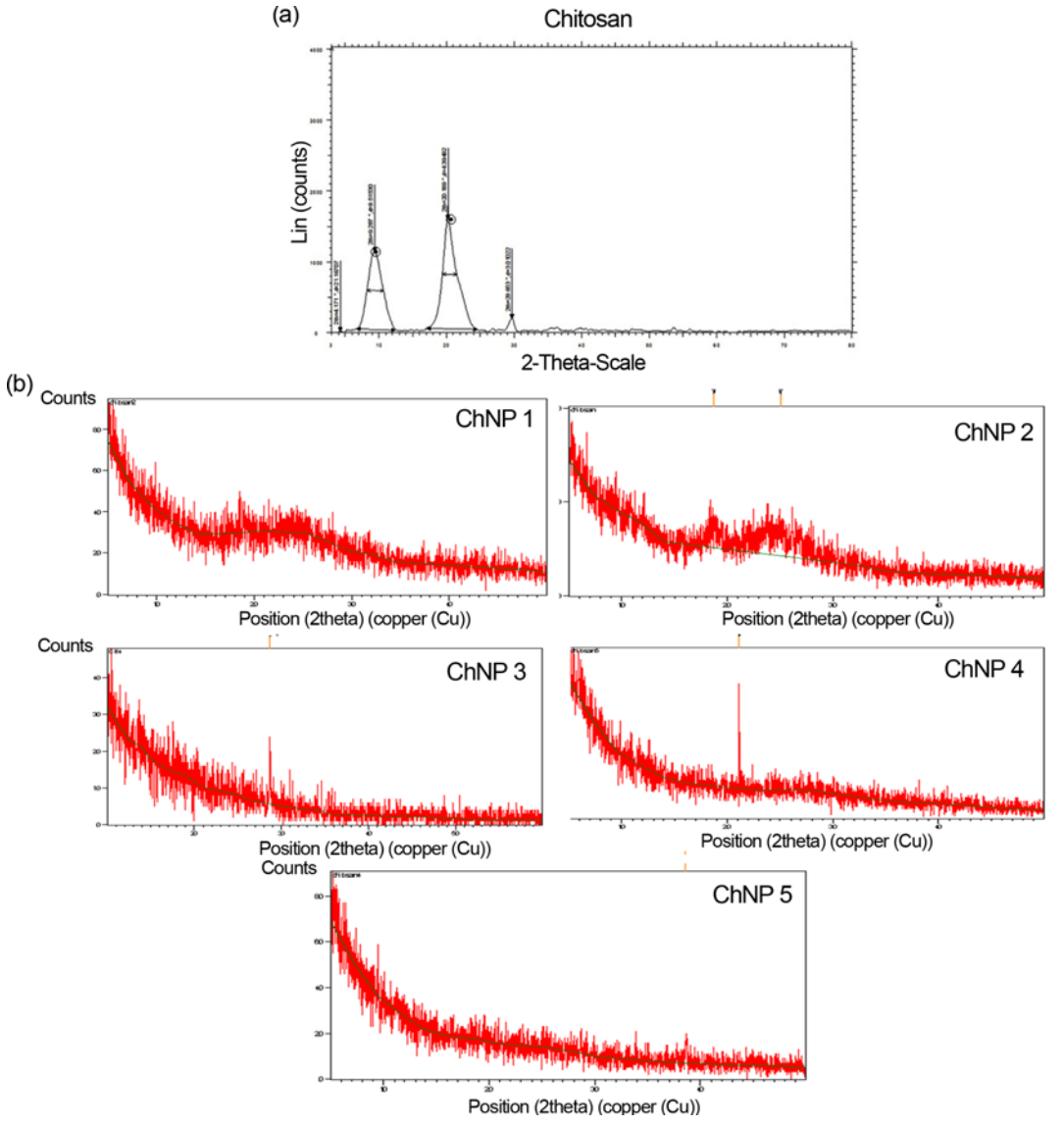

Figure 1. X-ray powder diffraction patterns of (a) Chitosan and (b) ChNP compounds 1 (1 mg/m*l*), 2 (2 mg/m*l*), 3 (3 mg/m*l*), 4 (4 mg/m*l*), 5 (5 mg/m*l*).

zone of inhibition of diameter 12 mm against *K. pneumoniae* while chitosan and chitin produced only 4 mm and 2.6 mm respectively. $ChNP_4$ produced a zone of inhibition of diameter 12 mm, 16 mm and 14 mm against *S. aureus, P. aeruginosa* and *E. coli* respectively. Chitosan and chitin only produced less than 8 mm against each pathogen.

Mechanism of Antibacterial Activity

Cell Membrane Integrity

The amount of intracellular material released from challenge microorganism treated with ChNP is shown in Figure 7. The absorption at 260 nm increased till 80 min and then decreased. The nucleic acid release was highest for $ChNP_3$ treated *K. pneumoniae*, while $ChNP_4$ showed the highest release for *S. aureus, P. aeruginosa* and *E. coli* had more nucleic acid release upon treatment with $ChNP_2$.

Factors Affecting Antibacterial Activity

Tetrazolium/Formazan Test (TTC Test)

The antibacterial activity of $ChNP_4$ and $ChNP_3$ against *K. pneumoniae* and *S. aureus* was evaluated using 2,3,5-triphenyl-2H-tetrazolium chloride (TTC). Figure 8 shows the antibacterial activity in relation to pH, temperature and reactive time. A strong reduction of vital cells in the presence of ChNP was observed. The presence of vital cells resulted in heavy red color due to the formation of triphenyl formazan (TPF) which turned pale yellow as a number of vital cells decreased. *K. pneumoniae* showed the highest

Table 2. Determination of the crystalline size of silver nanoparticles using Debye Scherrer's equation

Sample	2θ	β(radians)	d (nm)
ChNP1	25.35	0.07	19
ChNP2	25.01	0.06	21
ChNP3	27.57	0.03	120
ChNP4	21.13	0.02	165
ChNP5	38.60	0.01	153

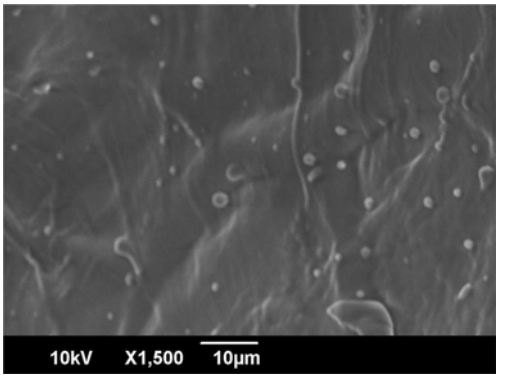

Figure 2. Scanning electron micrograph of chitosan nanoparticle.

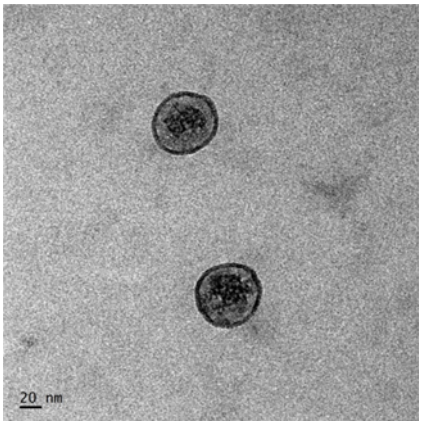

Figure 3. Transmission electron micrograph of chitosan nanoparticle.

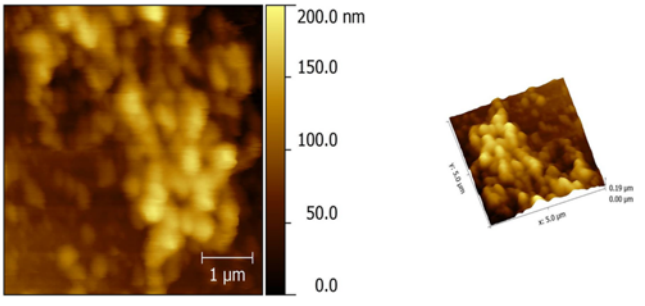

Figure 4. Atomic force micrographs (AFMs) of chitosan nanoparticle.

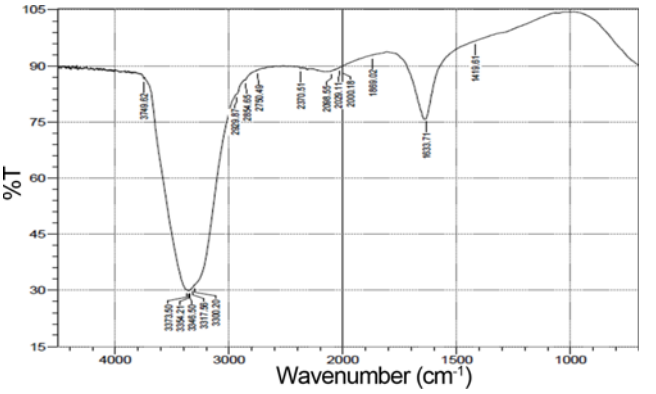

Figure 5. FTIR spectra of chitosan nanoparticle.

susceptibility at pH 7.5 and *S. aureus* at 5.5. Both bacteria were more susceptible at 37 °C. The absorption decreased along with reactive time indicating the decrease in number of vital cell with increased reaction time. The results are in accordance with previous results [30].

Biofilm Inhibition Assay

The antibiofilm activity of ChNP was determined using percent inhibition and MIC_{50} values. The MIC values were calculated from percent inhibition and further confirmed by growth on CRA plates. Compared to antibacterial activity, ChNP showed lower antibiofilm activity. ChNP inhibited 97 % of *E. coli* at 500 mg/m*l*, 96 % *K. pneumoniae* at 400 mg/m*l*, 85% *P. aeruginosa* at 500 mg/m*l* and 92 % *S. aureus* at 200 mg/m*l* (Table 5). The MIC_{50} of *E. coli, K. pneumoniae* and *S. aureus* was 100 mg/m*l*, but for *P. aeruginosa* it was 200 mg/m*l* (Figure 9). The glass beads grown in the MIC concentration produced no colonies when plated on CRA plates (Figure 10).

Discussion

Chitosan is the deacetylated form of chitin, an abundant polysaccharide. It has great commercial value due to its high nitrogen content and other physiochemical properties like biocompatibility, adsorptive ability etc. Chitosan nanoparticles have been reported to show increased activity than its parent chitosan due to increased surface to volume ratio of nanoparticles. In the present study, ChNP were synthesized and characterized and the antimicrobial activity of ChNP has been dealt in detail.

The particle size of ChNP is an important parameter that influences its antimicrobial activity. There are various factors affecting the particle size of nanoparticle like concentration, molecular weight of chitosan and so on [13]. The decrease in size at lower concentrations is due to decreased viscosity causing better solubility of chitosan in acetic acid solution thus allowing more amino groups on chitosan to be protonated causing better interaction with the

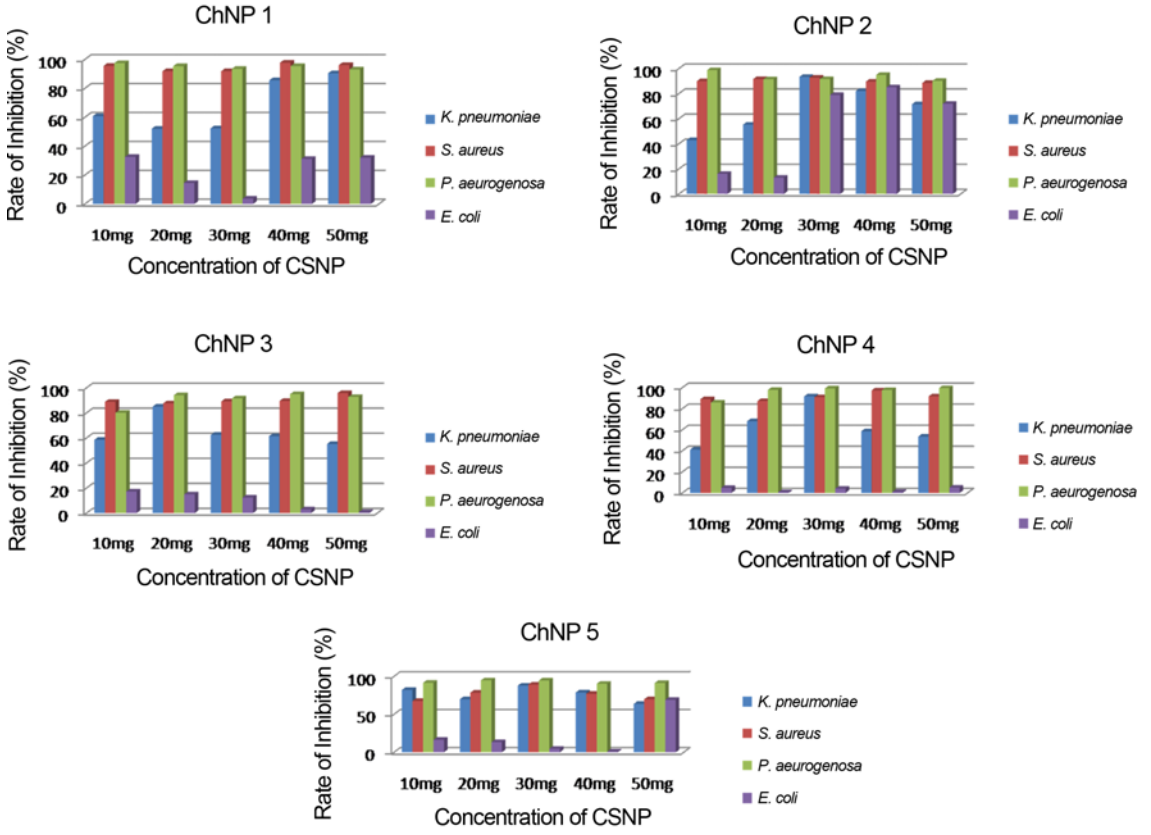

Figure 6. Effect of ChNP on inhibition of growth of microorganisms using OD_{600} measurements. Inhibition rate (%) calculated from equation (2) of each ChNP compounds 1 (1 mg/m*l*), 2 (2 mg/m*l*), 3 (3 mg/m*l*), 4 (4 mg/m*l*), 5 (5 mg/m*l*) against microorganism.

Table 3. Minimum inhibitory concentration of ChNP compounds 1 (1 mg/m*l*), 2 (2 mg/m*l*), 3 (3 mg/m*l*), 4 (4 mg/m*l*), 5 (5 mg/m*l*), chitosan (5 mg/m*l*), chitin (5 mg/m*l*) against selected bacteria

Sample	MIC (mg/m*l*)			
	K. pneumoniae	*S. aureus*	*P. aerogenosa*	*E. coli*
ChNP1	50	40	40	10
ChNP2	30	30	30	40
ChNP3	20	50	10	10
ChNP4	30	40	10	50
ChNP5	30	30	20	50

Table 4. Diameter of zone of inhibition of ChNP compounds 1 (1 mg/m*l*), 2 (2 mg/m*l*), 3 (3 mg/m*l*), 4 (4 mg/m*l*), 5 (5 mg/m*l*), chitosan (5 mg/m*l*), chitin (5 mg/m*l*) against selected bacteria

Sample	Zone of inhibition (mm)			
	K. pneumoniae	*S. aureus*	*P. aerogenosa*	*E. coli*
ChNP1	7.66	10.3	13	11
ChNP2	5.33	9.33	14	11.6
ChNP3	12	10	13.3	9.6
ChNP4	11.6	12.3	15.3	14
ChNP5	10.3	10.3	12.3	9.6
Chitosan	4	5	8.3	5.3
Chitin	2.6	6	7.6	8.3

polyanion [33].

X-ray spectroscopy is a widely used means of characterizing materials. In X-ray diffraction measurement, the sample is bombarded with X-rays and the diffraction pattern produced is recorded [34]. The two major peaks of chitosan are at 2θ= 9.9-10.7 and 19.8-20.7° [32,35]. These peaks can be observed for ChNP also [2]. In some cases, due to the transformation of structure to amorphous nature, a disappearance of the peak at 20° and appearance of broad bands at 2θ=35° has been reported [36].

The FTIR spectra of ChNP can be used to analyze the functional groups present. It works on the principle of vibrations of atoms of a molecule [34]. The FTIR spectra of ChNP commonly show a peak at around 3400 cm^{-1} that correspond to O-H stretching vibration in chitosan [37]. This peak is usually sharper for ChNP as compared to chitosan

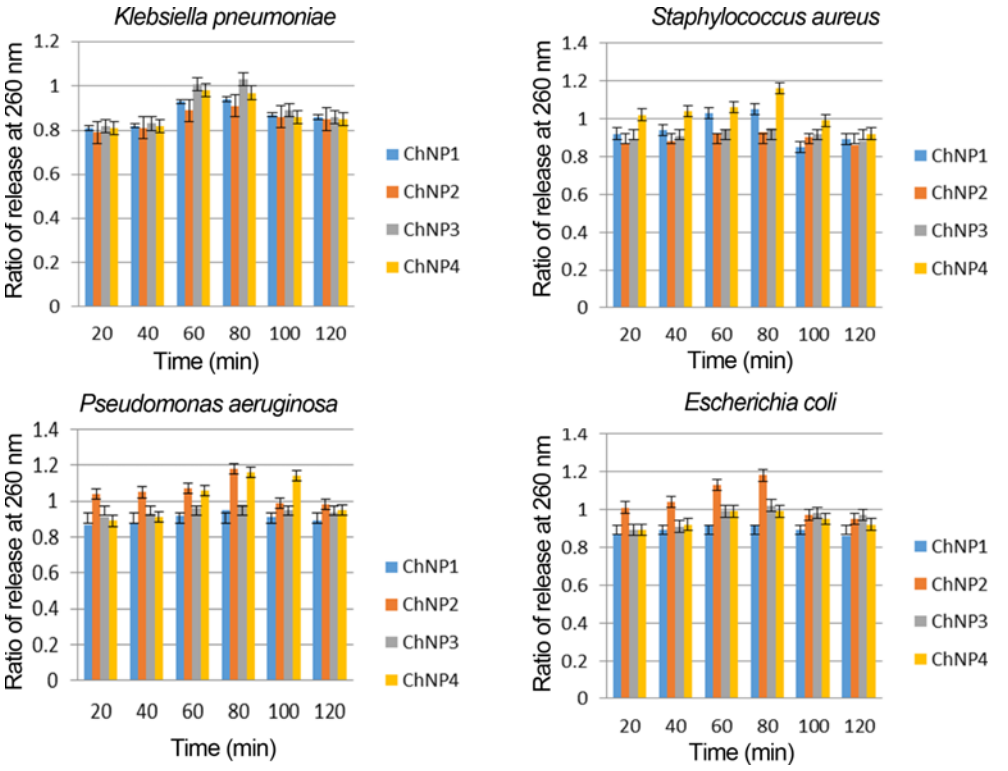

Figure 7. Ratio of release of cell contents analyzed by measuring absorption at 260 nm of ChNP compounds 1 (1 mg/m*l*), 2 (2 mg/m*l*), 3 (3 mg/m*l*), 4 (4 mg/m*l*), 5 (5 mg/m*l*), chitosan (5 mg/m*l*), chitin (5 mg/m*l*) treated *K. pneumoniae, S. aureus, P. aeruginosa* and *E. coli.*

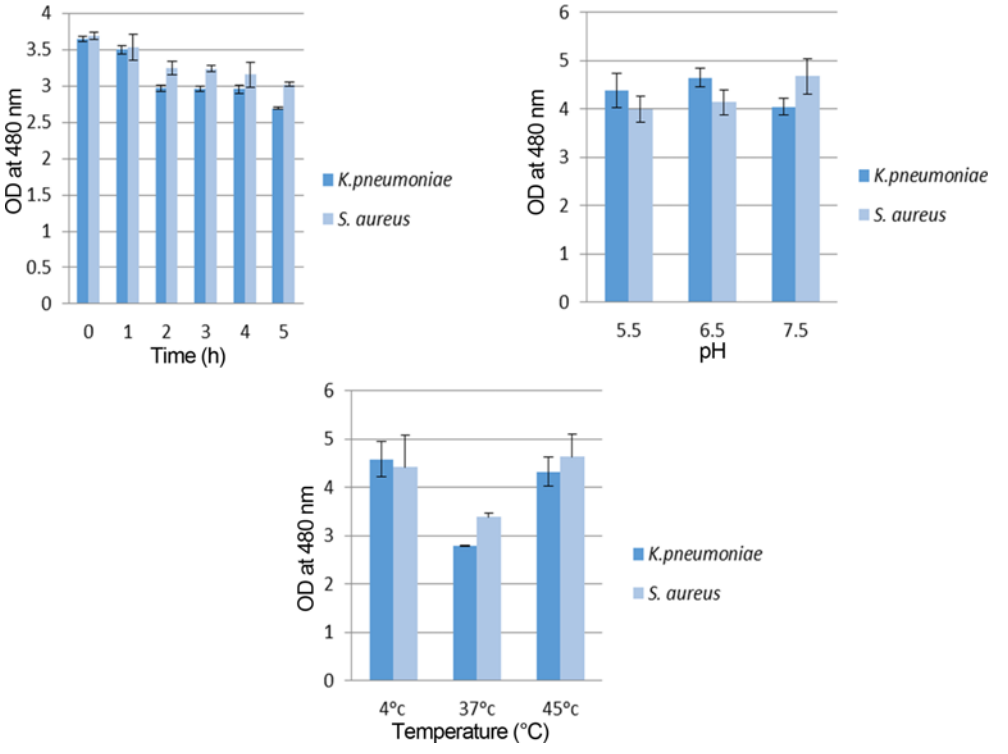

Figure 8. Antibacterial activity of ChNP compounds ChNP3 and ChNP4 against *K. pneumoniae* and *S. aureus* respectively with respect to pH, Temperature and Reactive time.

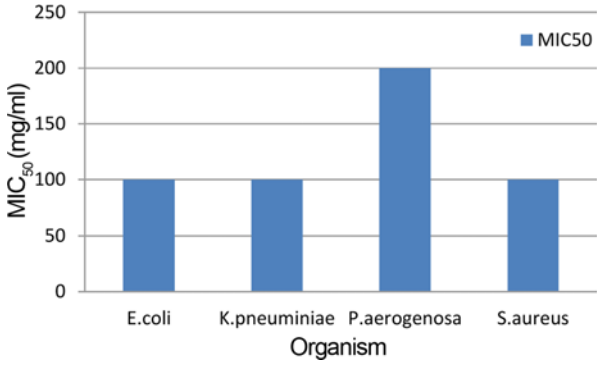

Figure 9. Minimum inhibitory concentration (MIC_{50}) of ChNP (100 mg/m*l*, 200 mg/m*l*, 300 mg/m*l*, 400 mg/m*l* and 500 mg/m*l*) against selected bacteria.

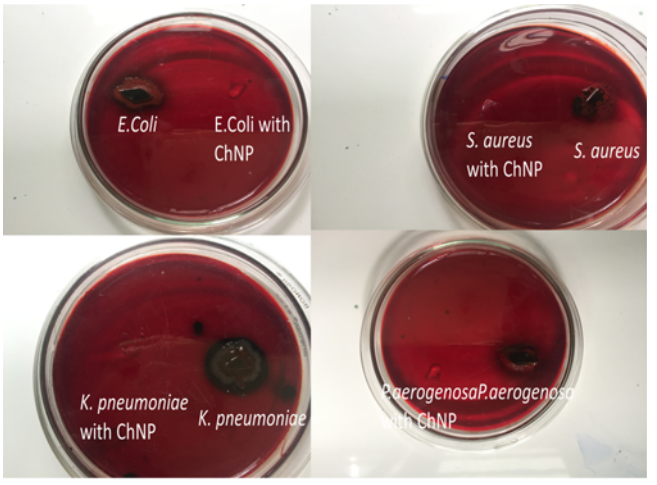

Figure 10. Congo red agar plates showing the antibiofilm activity of ChNP against *E. coli* at mg/m*l*, *K. pneumoniae* at mg/m*l*, *P. aeruginosa* at mg/m*l* and *S. aureus* at mg/m*l*.

Table 5. Percent of inhibition of CHNP compounds (100 mg/m*l*, 200 mg/m*l*, 300 mg/m*l*, 400 mg/m*l*, and 500 mg/m*l* against selected bacteria

Concentration of ChNP (mg/m*l*)	Percent inhibition			
	E. coli	*K. pneumoniae*	*P. aeruginosa*	*S. aureus*
100	54	57	46	76
200	56	58	50	92
300	58	79	59	94
400	65	96	79	97
500	97	94	85	98

indicating the enhanced hydrogen bonding of nanoparticles [17]. There is a shift in peak from 1650 and 1590 to 1630 and 1540 indicating the cross-linkage of ammonium groups with tripolyphosphate molecules. The polyphosphoric groups of TPP interacts with ammonium groups of chitosan thus enhancing the inter and intramolecular interaction of ChNP [38].

The microscopic assay of ChNP has shown it to be spherical in shape. This is due to the aggregation of chitosan and tripolyphosphate molecules. This gives it a low particle size and high specific surface energy [39].

ChNP were found to have higher antimicrobial activity than chitosan and chitin. This is due to the spherical character of NP. The polycationic ChNP interact with the negatively charged surface of bacteria to a greater degree than chitosan and chitin. Besides the large surface area of ChNP enables it to be tightly absorbed to the surface of bacteria thereby disrupting the membrane leading to leakage of intracellular compounds and subsequently cell death [17].

The bacterial membrane which serves as a structural compound might be compromised during exposure to ChNP. This causes leakage of intracellular molecules. Small ions like potassium and phosphate are first to leach out followed by large molecules like DNA, RNA etc. since these nucleotides have strong absorption at 260 nm, it can be detected using a UV/Vis spectrophotometer [40].

The tetrazolium/formazan couple is a redox system that enables quick evaluation of antibacterial activity of compounds. Bacteria reduce TTC to red triphenyl formazan. The intensity of the red color formed is directly proportional to the number of viable cells [30].

Chitosan nanoparticles were synthesized and characterized in the current study. The obtained nanoparticles had small particle size and efficient antibacterial activity. The mode of antibacterial action of ChNP was studied briefly and evidence of ChNP disrupting bacterial membrane causing cell death was obtained. The effect of various factors like pH, reactive time and temperature on the antibacterial activity of ChNP was studied. Further in vivo studies to demonstrate the nontoxicity of ChNP will allow for the use of ChNP as antibiotic agents.

Biofilm forming microorganisms is the major cause of prosthetic device related infections. Though it is a major medical problem, much work has not been done in this respect [43]. In the present study, ChNP were found to have antibiofilm activity, with an inhibition rate of up to 98 %. This is accordance with previous studies where 96 % inhibition of Streptococcus mutans has been reported [44]. The effect may be due to exopolysaccharide synthesis inhibition resulting in less biofilm formation [41]. Studies have also reported the diffusion of nanoparticles through the channels in biofilm [45].

Conclusion

Chitosan nanoparticles exhibit potential antibacterial activity as their unique character. Chitosan nanoparticles

showed promising antimicrobial activity against medically relevant microorganisms. $ChNP_4$ showed activity against *S. aureus, P. aeruginosa*, and *E. coli* while *K. pneumoniae* was inhibited by $ChNP_3$. It was also seen that chitosan nanoparticle had more activity than chitosan and chitin. The antibiofilm activity of nanoparticles has been studied and was found to be effective. Further study on the toxicity of chitosan nanoparticles is needed to establish it as an antimicrobial agent.

Acknowledgements

Authors convey thanks to School of Pure and Applied Physics, Mahatma Gandhi University for providing XRD. We would like to thank School of Chemical Sciences Mahatma Gandhi University Kerala for providing SEM. We thank DBT-MSUB, School of Biosciences, Mahatma Gandhi University for providing FT-IR. We also thank International and Inter University Centre for Nanoscience and Nanotechnology for providing AFM.

References

1. M. Raffi, S. Mehrwan, T. M. Bhatti, J. I. Akhter, A. Hameed, W. Yawar, and M. M. Ul Hasan, *Ann. Microbiol.*, **60**, 75 (2010).
2. M. S. Usman, M. E. El Zowalaty, K. Shameli, N. Zainuddin, M. Salama, and N. A. Ibrahim, *Int. J. Nanomed.,* **8**, 4467 (2013).
3. L. Didenko, D. Gerasimenko, N. Konstantinova, T. Silkina, I. Avdienko, G. Bannikova, and V. Varlamov, *B Exp. Biol. Med.,* **140**, 356 (2005).
4. M. E. I. Badawy and E. I. Rabea, *Int. J. Carbohydr. Chem.,* **2011**, 1 (2011).
5. S. Pangburn, P. Trescony, and J. Heller, *Biomaterials*, **3**, 105 (1982).
6. S. B. Rao and C. P. Sharma, *J. Biomed. Mater. Res.*, **34**, 21 (1997).
7. S. K. Kim and N. Rajapakse, *Carbohydr. Polym.*, **62**, 357 (2005).
8. Y. Okamoto, S. Minami, A. Matsuhashi, H. Sashiwa, H. Saimoto, Y. Shigemasa, T. Tanigawa, Y. Tanaka, and S. Tokura, *J. Vet. Med. Sci*., **55**, 743 (1993).
9. M. Thongngam and D. J. McClements, *J. Agri. Food Chem.*, **52**, 987 (2004).
10. I. Helander, E. L. Nurmiaho-Lassila, R. Ahvenainen, J. Rhoades, and S. Roller, *Int. J. Food Microbiol*., **71**, 235 (2001).
11. P. J. Park, J. Y. Je, and S. K. Kim, *Carbohydr. Polym*., **55**, 17 (2004).
12. Z. X. Tang, J. Q. Qian, and L. E. Shi, *Appl. Biochem. Biotechnol*., **136**, 77 (2007).
13. L. Yien, N. M. Zin, A. Sarwar, and H. Katas, *Int. J. Biomater,* **2012**, 1 (2012).
14. L. E. C. de Paz, A. Resin, K. A. Howard, D. S. Sutherland, and P. L. Wejse, *Appl. Environ. Microbiol*., **77**, 3892 (2011).
15. L. Huang, X. Cheng, C. Liu, K. Xing, J. Zhang, G. Sun, X. Li, and X. Chen, *Front. Biol.,* **4**, 321 (2009).
16. P. Kaur, A. Choudhary, and R. Thakur, *Int. J. Sci. Eng. Res.,* **4**, 869 (2013).
17. L. Qi, Z. Xu, X. Jiang, C. Hu, and X. Zou, *Carbohydr. Res*., **339**, 2693 (2004).
18. P. Kaur, R. Thakur, and A. Choudhary, *Int. J. Sci. Technol., Res.*, **1**, 83 (2012).
19. E. Russo, N. Gaglianone, S. Baldassari, B. Parodi, S. Cafaggi, C. Zibana, M. Donalisio, V. Cagno, D. Lembo, and G. Caviglioli, *Colloid Surf. B-Biointerfaces*, **118**, 117 (2014).
20. Y. Mori, T. Ono, Y. Miyahira, V. Q. Nguyen, T. Matsui, and M. Ishihara, *Nanoscale Res. Lett*., **8**, 88 (2013).
21. Y. C. Chung, Y. P. Su, C. C. Chen, G. Jia, H. I. Wang, J. G. Wu, and J. G. Lin, *Acta Pharmacol. Sin.*, **25**, 932 (2004).
22. X. Wang, Y. Du, and H. Liu, *Carbohydr. Polym.*, **56**, 21 (2004).
23. Z. Zhong, R. Xing, S. Liu, L. Wang, S. Cai, and P. Li, *Carbohydr. Res.*, **343**, 566 (2008).
24. A. Nagy, A. Harrison, S. Sabbani, R. S. Munson, Jr., P. K. Dutta, and W. J. Waldman, *Int. J. Nanomed.*, **6**, 1833 (2011).
25. R. Cuero, G. Osuji, and A. Washington, *Biotechnol. Lett*., **13**, 441 (1991).
26. M. Kong, X. G. Chen, K. Xing, and H. Park, *J. Int. J. Food Microbiol.*, **144**, 51 (2010).
27. P. Calvo, C. R. Lopez, J. L. V. Jato, and M. J. Alonso, *J. Appl. Polym. Sci.*, **63**, 125 (1997).
28. J. A. J. Nesalin and A. A. Smith, *Asian J. Pharm. Sci.,* **7**, 80 (2012).
29. A. Sarwar, H. Katas, and N. M. Zin, *J. Nanopart. Res.*, **16**, 1 (2014).
30. S. H. Moussa, A. A. Tayel, A. A. Al-Hassan, and A. Farouk, *J. Mycol.*, **2013**, 2517 (2013).
31. A. Tarafdar and G. Biswas, *Int. J. Theor. Appl. Res. Mech. Eng.*, **2**, 2319 (2013).
32. K. H. Prashanth, F. Kittur, and R. Tharanathan, *Carbohydr. Polym.*, **50**, 27 (2002).
33. H. Katas and H. O. Alpar, *J. Control Release,* **115**, 216 (2006).
34. J. Kumirska, M. Czerwicka, Z. Kaczynski, A. Bychowska, K. Brzozowski, J. Thoming, and P. Stepnowski, *Mar. Drugs,* **8**, 1567 (2010).
35. M. T. Yen, J. H. Yang, and J. L. Mau, *Carbohydr. Polym.*, **75**, 15 (2009).
36. X. Yin, X. Zhang, Q. Lin, Y. Feng, W. Yu, and Q. Zhang, *Arkivoc*, **9**, 66 (2004).
37. K. C. A. G. Annadurai, *J. Acad. Ind. Res.,* **1**, 4 (2012).
38. Y. Xu and Y. Du, *Int. J. Pharm*, **250**, 215 (2003).
39. U. K. Parida, N. Rout, and B. K. Bindhani, *Adv. Biosci. Biotechnol.*, **2013**, 1 (2013).
40. C. Z. Chen and S. L. Cooper, *Biomaterials,* **23**, 3359

(2002).
41. S. K. R. Namasivayam and E. A. Roy, *Int. J. Sci. Res. Publi.*, **3**, 591 (2013).
42. A. Hassan, J. Usman, F. Kaleem, M. Omair, A. Khalid, and M. Iqbal, *Braz. J. Infect. Dis.,* **15**, 305 (2011).
43. S. Moteeb, *Journal of University of Anbar for Pure Science*, **2**, 3 (2008).
44. L. E. C. de Paz, A. Resin, K. A. Howard, D. S. Sutherland, and P. L. Wejse, *Appl. Environ. Microbiol.*, **77**, 3892 (2011).
45. K. Kalishwaralal, S. B. Manikanth, S. R. Pandian, V. Deepak, and S. Gurunath, *Colloid Surf. B-Biointerfaces*, **79**, 340 (2010).